Switchable Molecules

DOI: 10.1002/ange.200500316

Reverse Spin Transition Triggered by a Structural Phase Transition**

Shinya Hayami, Yuji Shigeyoshi, Motoko Akita, Katsuya Inoue, Kenichi Kato, Keiichi Osaka, Masaki Takata, Ryo Kawajiri, Tadaoki Mitani, and Yonezo Maeda*

Designing molecules that could be used for information processing and information storage is one of the main challenges in molecular materials science. Molecules that are suitable for such applications must be bistable: a characteristic that allows the presence of two different stable electronic states over a certain range of external perturbation. Typical examples of molecular species that exhibit such bistability are the spin-crossover (SCO) compounds. Since the discovery of the first SCO compound,[1] a variety of d^n ($n = 4$–7) transition metal compounds exhibiting bistability between the high-spin (HS) and low-spin (LS) states have been reported.[2–4] Spin transition can be induced by variation of temperature, pressure, or illumination.[2–9] In general, temperature-dependent SCO behavior involves reversible spin transition from LS to HS upon heating and from HS to LS upon cooling.

Although the SCO transition is due to the electronic structure of the single molecule and can be observed even in

[*] Dr. S. Hayami, Y. Shigeyoshi, Prof. Dr. Y. Maeda
Department of Chemistry, Graduate School of Sciences
Kyushu University
6-10-1 Hakozaki, Higashi-ku, Fukuoka 812-8581 (Japan)
Fax: (+81) 92-642-2589
E-mail: hayascc@mbox.nc.kyushu-u.ac.jp
Dr. M. Akita
Institute for Molecular Science
Myodaiji, Okazaki 444-8585 (Japan)
Prof. Dr. K. Inoue
Department of Chemistry, Faculty of Science
Hiroshima University
1-3-1 Kagamiyama, Higashi-hiroshima 739-8526 (Japan)
Dr. K. Kato, Dr. K. Osaka, Prof. Dr. M. Takata
JASRI/SPring-8
1-1-1 Kouto, Mikazuki-cho, Sayo-gun, Hyogo 679-5198 (Japan)
R. Kawajiri, Prof. Dr. T. Mitani
Japan Advanced Institute of Science and Technology
Tatsunokuchi, Ishikawa 923-1292 (Japan)

[**] This work was supported by the Tokuyama Foundation, the Ogasawara Foundation, and the Research and Education Grant-in-Aid of IEI-J. The synchrotron radiation X-ray powder diffraction experiments were performed at the SPring-8 BL02B2 beam line with approval of the Japan Synchrotron Radiation Research Institute (JASRI). We thank Dr. Y. Kawashima and Dr. Y. Otsuka for their help in reviewing this contribution, as well as Prof. A. Mori and Prof. S. Ujiie for helpful suggestions for thermal analysis.

Supporting information for this article is available on the WWW under http://www.angewandte.org or from the author.

 © 2005 Wiley-VCH Verlag GmbH & Co. KGaA, Weinheim

solutions or polymer matrices,[10,11] interaction between SCO molecules can dramatically influence the transition. Gradual or abrupt spin transitions may be observed in the solid state, depending on cooperativity.[12–14] The understanding of cooperative behavior in SCO transition can be a key to designing materials that are useful for information technology. In contrast, flexibility in the synthesis of molecular assemblies based on molecular units is also very important for synergy among the various interesting and novel physical properties of advanced materials.[15,16] The flexibility of ligands is one factor that can both directly and indirectly influence the cooperative interaction. The direct influence arises from the structural changes of the ligands, and the indirect influence comes from their random packing structure.

The SCO cobalt(II) compounds exhibit a 1/2↔3/2 spin change. The cobalt(II) compounds $[Co(terpy)_2]X_2 \cdot n\,H_2O$ (terpy = 2,2′:6′,2″-terpyridine; X = halide, pseudohalide, NO_3^-, ClO_4^-; $n = 0$–5) exhibit incomplete and gradual SCO behavior.[17,18] Not only liquid-crystal properties, but also unique physical properties can be expected for compounds with long alkyl chains because of the thermal motion of the alkyl chains. On the basis of these observations, we prepared cobalt(II) compounds with long alkyl chains and succeeded in observing "reverse spin transition" by using a major structural phase transition for the first time. Notably, reverse spin transition is unexpected because the driving force of the SCO phenomenon is entropy change, which is temperature-dependent.

The focus of the work reported herein was the cobalt(II) compound $[Co(C_{16}\text{-terpy})_2](BF_4)_2$ (**1**, in which C_{16}-terpy = 4′-hexadecyloxy-2,2′:6′,2″-terpyridine) having terpy ligands with long alkyl chains. Unsolvated **1** was obtained as a brown–orange powder by treating a solution of $Co^{II}(BF_4)_2$ in methanol with 2 equiv C_{16}-terpy. Single crystals of **1**·MeOH suitable for X-ray diffraction (XRD) studies were isolated by slow recrystallization from MeOH. The compound crystallizes in triclinic space group $P\bar{1}$. The cobalt(II) ion of **1**·MeOH is octahedrally coordinated by six nitrogen atoms of two C_{16}-terpy ligands (Figure 1). The bond lengths are intermediate between those of typical LS and HS cobalt(II) compounds.[19] The Co–N distances of the central pyridine ring of the terpyridine ligand (1.99 Å) are shorter than those of the peripheral pyridine rings (2.13 Å), and this induces a pronounced distortion of the CoN_6 octahedron. The three pyridine rings of the C_{16}-terpy ligand are coplanar, and the two tridentate C_{16}-terpy ligands are nearly perpendicular to one another. The long alkoxy chains $C_{16}H_{33}O$ form rodlike structures that protrude from the 4′-positions of the terpyridine moieties. The chain from O1 extends straight in zig-zag form, whereas the other is bent at C48–C49 and then extends straight in a zig-zag fashion. The thermal motions of the end carbon atoms C60, C61, and C62 of the long chain connected to O2 are larger than those of C29, C30, and C31 in the O1 chain. The two BF_4^- counteranions and one MeOH molecule are located in the intermolecular space, and there are short contacts between $[Co(C_{16}\text{-terpy})_2]^{2+}$ cations, BF_4^- anions, and MeOH molecules. The $[Co(C_{16}\text{-terpy})_2]^{2+}$ cations form short contacts (3.49 Å) between nearest-neighbor peripheral pyridine rings in the *ab* plane, and thus a 2D sheet is formed by π–π interactions. Furthermore, a fastener effect is present between the chains which face each other in the complexes. The very tight molecular packing of the compound suggests the presence of strong intermolecular interactions in the molecular assembly.

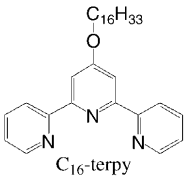

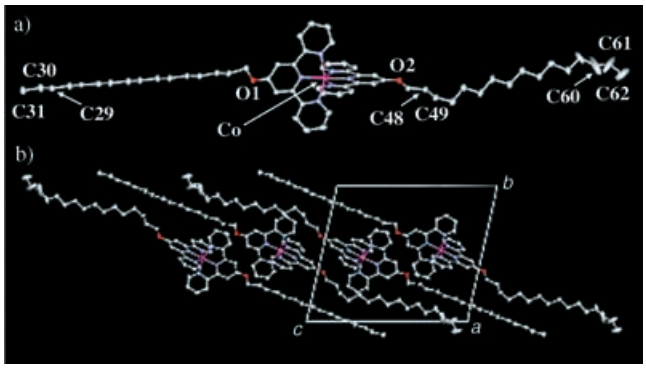

Figure 1. a) ORTEP plot of **1**·MeOH showing 50% probability displacement ellipsoids. b) Projection of the crystal structure of **1**·MeOH on the *bc* plane; BF_4^- ions, MeOH molecules, and H atoms are omitted for clarity.

The crystal structure of unsolvated **1** could not be determined, because the removal of MeOH induced cracks in the crystal that made single-crystal XRD studies impossible. However, powder XRD data suggested that the structure of unsolvated **1** is similar to that of **1**·MeOH (Supporting Information).

The temperature dependence of the molar magnetic susceptibility of unsolvated **1** is shown in Figure 2a. Solvated **1**·MeOH exhibited gradual SCO behavior in the temperature range of 5–360 K. The $\chi_m T$ value of **1**·MeOH gradually increases from 0.54 to 1.83 $cm^3 K mol^{-1}$ at 360 K, and then decreases to 1.58 $cm^3 K mol^{-1}$ at 400 K from the removal of MeOH. Unsolvated **1** was obtained by annealing **1**·MeOH at 400 K. The $\chi_m T$ value of **1** gradually decreases from 1.58 $cm^3 K mol^{-1}$ at 400 K to 0.41 $cm^3 K mol^{-1}$ at 226 K, and the gradual decrease in the $\chi_m T$ value shows normal thermal SCO behavior. Upon further cooling, the $\chi_m T$ value increases abruptly at around $T_{1/2}\downarrow = 217$ K to 2.01 $cm^3 K mol^{-1}$ at 206 K. The magnetic behavior shows that compound **1** exhibits reverse spin transition from the LS to the HS state upon cooling. Upon heating, $\chi_m T$ undulates between 1.70 and 2.15 $cm^3 K mol^{-1}$ in the temperature range of 5–251 K. Undulating magnetic behavior is also unusual and difficult to understand. It may be caused by structural changes. Powder XRD measurements showed that the structure at 50 K is different from that at 130 K ($2\theta = 8.8$, 11.9, 13.2, and 14.8°; Figure 3a). With further heating, the $\chi_m T$ value abruptly drops at around $T_{1/2}\uparrow = 260$ K with transition from the HS to the LS state. Then the $\chi_m T$ value gradually increases in the temperature range of 267–400 K. The wide thermal hysteresis loop ($\Delta T = 43$ K) remained unchanged in successive thermal cycles, and this confirms that compound **1** exhibits reverse spin transition. This is important because an abrupt transition

 © 2005 Wiley-VCH Verlag GmbH & Co. KGaA, Weinheim

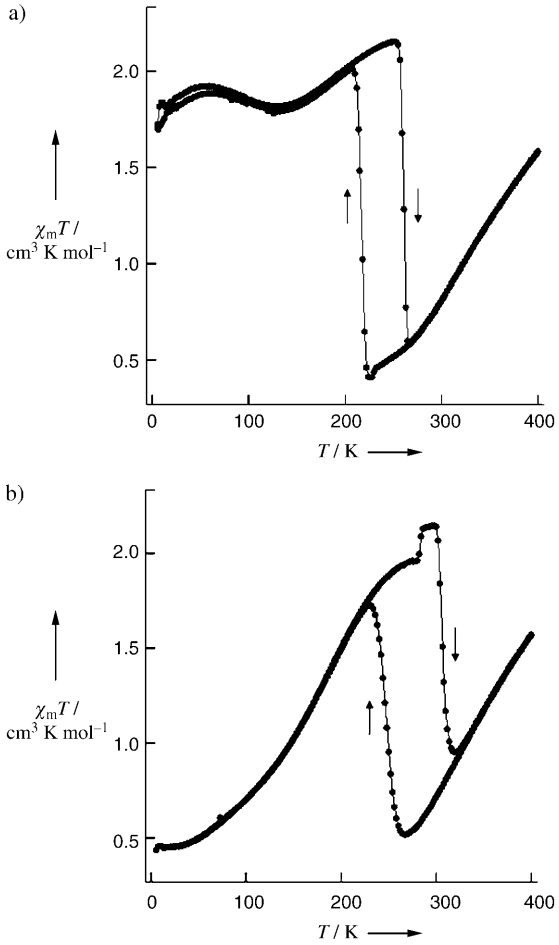

Figure 2. $\chi_m T$ versus T plots for a) **1** and b) **2**.

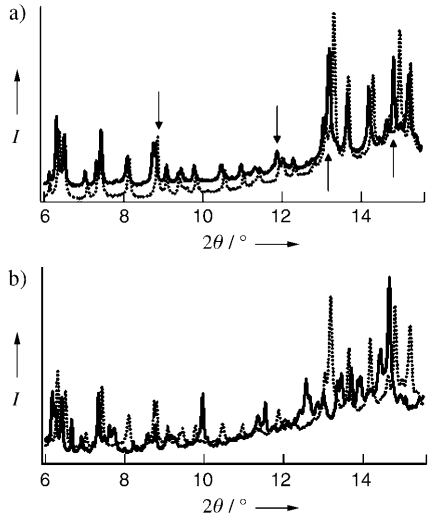

Figure 3. Temperature dependence of powder XRD patterns for **1** upon heating: a) (•••••): 50 K, (——): 130 K; b) (•••••): 130 K, (——): 270 K.

with a hysteresis loop appears only if the cooperative effect is strong enough. To confirm reverse spin transition, the variable-temperature ESR spectrum of **1** was measured. The spectrum shows a signal for the HS form at 3 K, and a signal for the LS form at 270 K. Powder XRD measurements show that the HS structure at 130 K differs greatly from the LS structure at 270 K, and a major structural phase transition is thought to occur in this temperature range (Figure 3b).

Upon warming, the reverse spin transition from the HS to the LS state ($T_{1/2}\uparrow = 260$ K) was found to be an endothermic phase transition ($\Delta H = 14.3$ kJ mol^{-1}, $\Delta S = 54.6$ J K^{-1} mol^{-1} at 262 K) by differential scanning calorimetry (DSC, Figure 4a).

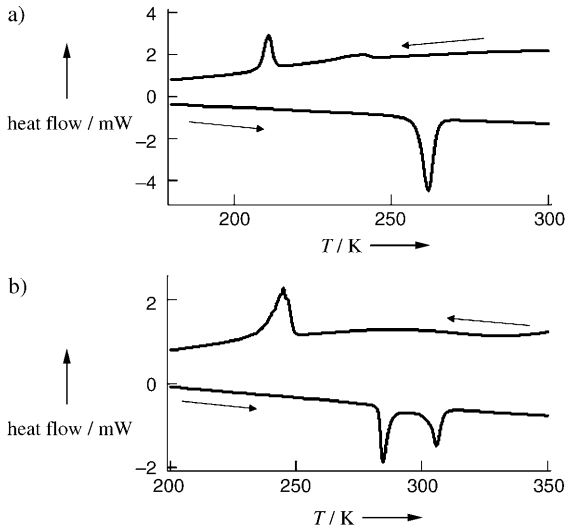

Figure 4. a) DSC curves of **1**. b) DSC of **2**.

Upon cooling, two peaks were observed, one at 211 K ($\Delta H = -6.1$ kJ mol^{-1}, $\Delta S = -28.6$ J K^{-1} mol^{-1}) and a broad peak at higher temperature. The exothermic peak at 211 K corresponds to the reverse spin transition temperature ($T_{1/2}\downarrow = 217$ K), and the broad peak can be assigned to another structural change. The sum of the two heat capacities upon cooling is equal to that of the peak at 262 K on heating. It has been reported that the change in entropy is 16–35 J mol^{-1} K^{-1} in SCO cobalt(II) compounds, and 40–65 J mol^{-1} K^{-1} in SCO iron(II) compounds.[7,18–21] The ΔS value for reverse spin transition ($\Delta S = 54.6$ J K^{-1} mol^{-1}) is larger than those previously reported for SCO cobalt(II) compounds, and is in the range of those observed in SCO iron(II) compounds ($\Delta S = 40$–65 J K^{-1} mol^{-1}). The ΔS value of **1** is much larger than the change in electronic spin expected for a cobalt(II) ion ($\Delta S_{spin} = R[\ln(2S+1)_{HS} - \ln(2S+1)_{LS}] = 5.8$ J K^{-1} mol^{-1}). The remaining entropy difference of 48.8 J K^{-1} mol^{-1} is mainly due to intramolecular vibrational changes. Furthermore, the iron(II) SCO compound $[Fe(ptz)_6](BF_4)_2$ (ptz = 1-propyltetrazole) undergoes spin transition with a structural phase transition from $R\bar{3}$ in the HS state to $P\bar{1}$ in the LS state, as deduced from powder diffraction experiments.[22] In such cases, the observed hysteresis is only the result of cooperative effects, as it is well-known that a first-order phase transition is generally accompanied by a hysteresis loop. We suggest that the major structural change in **1** is the origin of the reverse spin transition.

A similar compound, $[Co(C_{14}\text{-terpy})_2](BF_4)_2$ (**2**), which was synthesized by an analogous method, also exhibited reverse spin transition (Figure 2b). The $\chi_m T$ value of **2**

 © 2005 Wiley-VCH Verlag GmbH & Co. KGaA, Weinheim

gradually decreases from 1.57 $cm^3 K mol^{-1}$ at 400 K to 0.52 $cm^3 K mol^{-1}$ at 268 K, and then abruptly increases around $T_{1/2}\downarrow = 250$ K to 1.73 $cm^3 K mol^{-1}$ at 230 K. The magnetic behavior also shows that compound **2** exhibits reverse spin transition from the LS to the HS state upon cooling. With further cooling, the $\chi_m T$ value gradually decreases to 0.44 $cm^3 K mol^{-1}$ at 5 K which is normal SCO behavior. On heating, $\chi_m T$ value gradually increases to 1.96 $cm^3 K mol^{-1}$ at 280 K, and a jump in $\chi_m T$ from 1.96 $cm^3 K mol^{-1}$ to 2.15 $cm^3 K mol^{-1}$ was observed at 298 K. Upon further heating, $\chi_m T$ abruptly decreases, and shows the features of reverse spin transition from the HS to the LS state at $T_{1/2}\uparrow = 307$ K to 0.95 $cm^3 K mol^{-1}$ at 320 K. Then $\chi_m T$ gradually increases up to 400 K. The thermal hysteresis loop ($\Delta T = 57$ K) remained unchanged in successive thermal cycles, and thus confirmed that **2** exhibits reverse spin transition. An important characteristic of the present phenomenon is the wide hysteresis loop of 57 K. Furthermore, we emphasize that room temperature lies within the hysteresis loop.

Upon cooling, one peak was observed at 245 K ($\Delta H = -9.9$ kJ mol^{-1}, $\Delta S = -30.3$ J $K^{-1} mol^{-1}$), corresponding to a reverse spin transition from the LS to the HS state at $T_{1/2}\downarrow = 250$ K. Upon warming, two peaks were observed for **2** up to 400 K, at 284 K ($\Delta H_1 = 3.3$ kJ mol^{-1}, $\Delta S_1 = 11.5$ J $K^{-1} mol^{-1}$), and 306 K ($\Delta H_2 = 3.3$ kJ mol^{-1}, $\Delta S_2 = 10.8$ J $K^{-1} mol^{-1}$) by DSC (Figure 4b). The peak at 284 K corresponds to the jump in $\chi_m T$ in the magnetic data. Powder XRD measurements showed that the pattern at 280 K differs greatly from that at 300 K, and it is thought that a major structural phase transition occurs in this temperature range (Figure 5a). The second peak at 306 K corresponds to reverse spin transition from the HS to the LS state at $T_{1/2}\uparrow = 306$ K. The ΔS value for reverse spin transition ($\Delta S = 30.3$ J $K^{-1} mol^{-1}$) is in the range of those observed in other SCO Co^{II} compounds.[18–21] The powder XRD pattern at 300 K differs greatly from that at 350 K (Figure 5b). The jump in $\chi_m T$ and the reverse spin transition are thought to be accompanied by a major structural change.

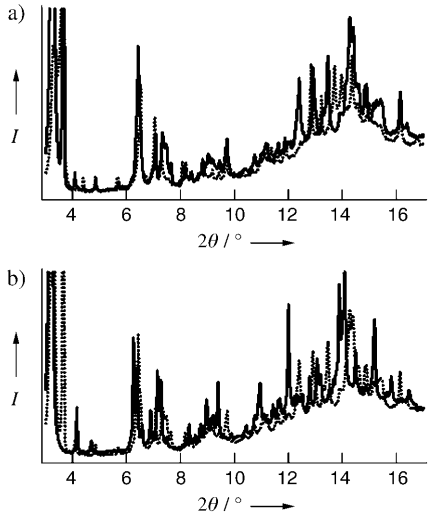

Figure 5. Temperature dependence of powder XRD patterns for **2** upon heating: a) (••••): 280 K, (——): 300 K; b) (••••):300 K, (——): 350 K.

Upon further heating, additional phase transitions due to the long alkyl chains were observed for **1** and **2** above 400 K by DSC (Supporting Information). Two peaks were observed for **1** at 437 and 512 K upon heating. The DSC peak at 437 K ($\Delta S = 33.9$ J $K^{-1} mol^{-1}$) can be assigned to a crystal–mesophase or crystal–crystal transition, and the peak at 512 K ($\Delta S = 17.7$ J $K^{-1} mol^{-1}$) can be assigned to the melting point. It is difficult to determine whether **1** exhibits mesophase transition. Two peaks were also observed for **2** at 443 K and 520 K upon heating. The DSC peak at 443 K ($\Delta S = 18.8$ J $K^{-1} mol^{-1}$) can be assigned to a crystal–crystal transition, and the peak at 520 K is assigned to the melting point.

Finally, we comment on the reverse spin transition observed in unsolvated compounds **1** and **2**. The molecular arrangement shows short contacts between $[Co(C_{16}\text{-terpy})_2]^{2+}$ cations, BF_4^- anions, and MeOH molecules, as well as between the long alkyl chains. The short contact distances are shorter than the sum of the van der Waals radius. Therefore, intermolecular interactions are strong and SCO behavior becomes cooperative. In such a case, the spin transitions between the HS and LS states are not only very abrupt, but also occur with hysteresis. The structural phase transitions that occur for **1** and **2** are likewise the result of strong intermolecular interactions. When one phase at low temperature prefers the HS state and another at high temperature prefers the LS state, reverse spin transition may be triggered by structural phase transitions.

In summary, we have synthesized $[Co(C_n\text{-terpy})_2](BF_4)_2$ ($n = 0$–22) with novel organic ligands based on a terpyridine frame. Compounds **1** and **2** with long alkyl chains exhibit reverse spin transition, which has been observed for compounds in which $n = 12$–16 so far. The reverse spin transitions have wide thermal hysteresis, which is important in switchable molecules. Thus, novel physical properties that could be important to the field of materials science may be discovered in compounds with long alkyl chains.

Experimental Section

1·MeOH: C_{16}-terpy (170 mg, 0.36 mmol) was dissolved in $CHCl_3$/MeOH (1:1, 20 mL) and added to a solution of $Co(BF_4)_2 \cdot 6H_2O$ (60 mg, 0.18 mmol) in MeOH (10 mL). The brown–orange solution was concentrated to ≈10 mL, and the resulting microcrystals were collected by filtration and recrystallized slowly from MeOH. Yield: 94 mg (43%); brown-orange crystals. Elemental analysis (%) calcd for $C_{63}H_{90}O_3N_6B_2F_8Co$: C 62.43, H 7.48, N 6.93, Co 4.86; found: C 62.48, H 7.53, N 6.98, Co 4.93. Elemental analysis (%) for **1** after removal of MeOH calcd for $C_{62}H_{86}O_2N_6B_2F_8Co$: C 63.11, H 7.35, N 7.12, Co 4.99; found: C 63.21, H 7.42, N 7.20, Co 4.83.

Crystallographic data for **1**·MeOH at 130 K ($C_{63}H_{90}O_3N_6B_2F_8Co_1$): $M_r = 1211.98$, brown–orange platelet ($0.35 \times 0.35 \times 0.15$ mm^3), triclinic, space group $P\bar{1}$, $a = 9.0412(6)$, $b = 17.598(1)$, $c = 20.684(2)$ Å, $\alpha = 102.545(3)$, $\beta = 101.622(3)$, $\gamma = 90.470(3)°$, $V = 3141.9(4)$ $Å^3$, $Z = 2$, $\rho_{calcd} = 1.281$ g cm^{-3}. Refinement by full-matrix least-squares methods gave an R factor of 0.08 from 9255 reflections with intensity $I > 3\sigma(I)$ for 748 variables; linear absorption coefficient $\mu(Mo_{K\alpha}) = 3.46$ cm^{-1}. Non-hydrogen atoms were refined anisotropically. Hydrogen atoms were included but not refined.

The magnetic susceptibilities $\chi(T)$ were measured between 5 and 300 K with a superconducting quantum interference device (SQUID) magnetometer (Quantum Design MPMS-5S) in an external field of 0.5 T. EPR spectra were recorded on a Bruker ESP 300 X-band (9.4 GHz) spectrometer equipped with a Hewlett-Packard 5350B

 © 2005 Wiley-VCH Verlag GmbH & Co. KGaA, Weinheim

microwave-frequency counter. Thermogravimetric data for **1** and **2** were collected on a Perkin-Elmer DSC-6 instrument over the temperature range of 290–450 K under an N_2 atmosphere.

To obtain X-ray powder diffraction data with good statistics and high angular resolution, XRD measurements were carried out at SPring-8, BL02B2 beam line (temperature dependence and illumination effect). The as-grown sample powders were sufficiently fine and gave a homogeneous intensity distribution in the Debye–Scherrer powder ring. At the BL02B2 beam line, the sample powders were sealed in glass capillaries in which the temperature was controlled in the range of 20–300 K. Reflections were collected on an imaging plate installed on a large Debye–Scherrer camera ($r = 286.5$ nm). The wavelength of the incident X-rays was ≈ 1.0 Å (slightly below the K edge of Rb), and typical exposure time was 15 min. The true wavelength was calibrated by using a standard CeO_2 powder obtained from NIST.

Received: January 27, 2005
Revised: March 5, 2005
Published online: July 11, 2005

Keywords: cobalt · magnetic properties · N ligands · spin crossover · tridentate ligands

[1] L. Cambi, A. Cagnasso, *Atti Accad. Naz. Lincei Cl. Sci. Fis. Mat. Nat. Re* **1931**, *53*, 809.
[2] P. Gütlich, Y. Garcia, H. A. Goodwin, *Chem. Soc. Rev.* **2000**, *29*, 419.
[3] J. A. Real, A. B. Gaspar, V. Niel, M. C. Munoz, *Coord. Chem. Rev.* **2003**, *236*, 121.
[4] J.-F. Letard, G. Chastanet, O. Nguyen, S. Marcen, M. Marchivie, P. Guionneau, D. Chasseau, P. Güetlich, *Monatsh. Chem.* **2003**, *134*, 165.
[5] W. S. Hammack, A. J. Conti, D. N. Hendrickson, H. G. Drickamer, *J. Am. Chem. Soc.* **1989**, *111*, 1738.
[6] S. Hayami, Y. Hosokoshi, K. Inoue, Y. Einaga, O. Sato, Y. Maeda, *Bull. Chem. Soc. Jpn.* **2001**, *74*, 2361.
[7] P. Gütlich, A. Hauser, H. Spiering, *Angew. Chem.* **1994**, *33*, 2109; *Angew. Chem. Int. Ed. Engl.* **1994**, *33*, 2024.
[8] S. Hayami, Z.-z. Gu, Y. Einaga, Y. Kobayasi, Y. Ishikawa, Y. Yamada, A. Fujishima, O. Sato, *Inorg. Chem.* **2001**, *40*, 3240.
[9] S. Hayami, Z.-z. Gu, M. Shiro, Y. Einaga, A. Fujishima, O. Sato, *J. Am. Chem. Soc.* **2000**, *122*, 7126.
[10] M. F. Tweedle, L. J. Wilson, *J. Am. Chem. Soc.* **1976**, *98*, 4824.
[11] A. Hauser, J. Adler, P. Gütlich, *Chem. Phys. Lett.* **1988**, *152*, 468.
[12] J.-F. Létard P. Guionneau, E. Codjovi, O. Lavastre, G. Bravic, D. Chasseau, O. Kahn, *J. Am. Chem. Soc.* **1997**, *119*, 10861.
[13] J. A. Real, E. Andrés, M. C. Muñoz, M. Julve, T. Granier, A. Bousseksou, F. Varret, *Science* **1995**, *268*, 265.
[14] A. J. Conti, C. L. Xie, D. N. Hendrickson, *J. Am. Chem. Soc.* **1989**, *111*, 1171.
[15] Y. Galyametdinov, V. Ksenofontov, A. Prosvirin, I. Ovchinnikov, G. Ivanova, P. Gütlich, W. Haase, *Angew. Chem.* **2001**, *113*, 4399; *Angew. Chem. Int. Ed.* **2001**, *40*, 4269.
[16] T. Fujigaya, D.-L. Jiang, T. Aida, *J. Am. Chem. Soc.* **2003**, *125*, 14690.
[17] J. S. Judge, W. A. Baker, Jr., *Inorg. Chim. Acta* **1967**, *1*, 68.
[18] S. Kremer, W. Henke, D. Reinen, *Inorg. Chem.* **1982**, *21*, 3013.
[19] A. B. Gaspar, M. C. Munoz, V. Niel, J. A. Real, *Inorg. Chem.* **2001**, *40*, 9.
[20] J. Zarembowitch, R. Claude, O. Kahn, *Inorg. Chem.* **1985**, *24*, 1576.
[21] J. Faus, M. Julve, F. Lloret, J. A. Real, J. Sletten, *Inorg. Chem.* **1994**, *33*, 5535.
[22] L. Wiehl, H. Spiering, P. Gütlich, K. Knorr, *J. Appl. Crystallogr.* **1990**, *23*, 151.

 © 2005 Wiley-VCH Verlag GmbH & Co. KGaA, Weinheim